Engineering Practice

Predict and Prevent Air Entrainment in Draining Tanks

The proper use of vortex breakers at tank outlets can prevent entrained vapors from flowing downstream

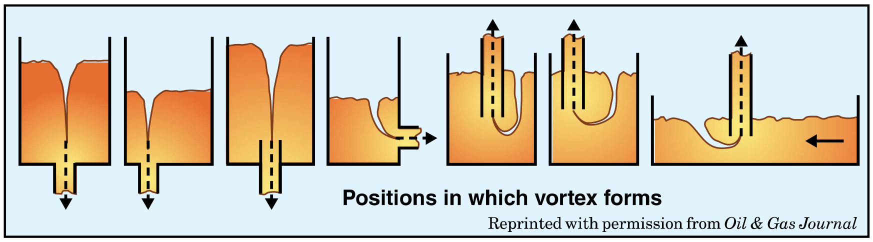

FIGURE 1. Various vortex configurations can form in draining tanks. They vary by tank geometry and the position of the drainage outlet (from Patterson [*1*])

Steve G. Rochelle
and **Marvin T. Briscoe, Jr.**
Eastman Chemical Co.

When tanks are draining, the potential may exist for a swirling vortex to form leading from the liquid surface to any of the bottom-exit or side-exit nozzles connected to downstream piping (Figure 1). One important aspect of the vortex is whether it will entrain air or other gases into the discharge flow. Such vapor entrainment can lead to a host of problems, ranging from vacuum collapse of the supply tank, to over-pressurization of the receiving tank, to a disruption of the vapor seal between the tanks. Meanwhile, if the entrained vapor is allowed to collect into pockets in elevated pipe loops, it can lead to two-phase flow, which can form liquid slugs that could damage downstream equipment. Similarly, if the flow from the tank is to the suction inlet of a pump, these gas pockets may result in surging, stalling (air-locking) or vane erosion. During continuous operations, such as when a tank is being filled and emptied at the same rate, or when a reboiler is being operated on the side of a column, vapor entrainment may cause pulsating or inconsistent flow.

According to publications available in the open literature, a variety of "vortex breaker" designs have been suggested and are reviewed below. When placed over the tank drain, they help to block or prevent the formation of vortexes. However, what is missing from the literature is useful guidance on when to use a vortex breaker. In general, vortex breakers should also be used judiciously to reduce capital and maintenance costs, and because they may be susceptible to fouling or plugging by solids.

Later, this article presents design information and rules-of-thumb for avoiding gas entrainment that have been gathered from the literature. It also provides several expanded design charts to help users both determine when the potential for vapor entrainment could arise, and evaluate various operating conditions or proposed tank and piping design choices.

Vortex breaker designs

Eastman Chemical Co. (the authors' employer) uses the vortex breaker design from Process Industry Practices (PIP) [*2*], as the company standard. This vortex breaker design relies on a baffle arrangement, either flush with the bottom of the tank, or suspended just off the tank bottom if the nozzle extends above the tank bottom. Figure 2 shows a 4-bladed design. For typical applications, the dimensions are expressed as a function of the diameter of the discharge nozzle (D), with the overall width of the device being $2D$, and the height of the blades equal to D, as shown.

Another vortex breaker design (from Patterson [*1*]) is shown in Figure 3. On the left is Patterson's circular plate of diameter $4D$, used for tanks with bottom drainage. It is suspended a distance of $D/2$ off the bottom. Shown at right is Patterson's design for tanks using vertical-suction pipes. It uses a circular solid plate with a $4D$ diameter to block vortexes from the surface.

Megyesy [*3*], who references Patterson [*1*], shows 2- and 4-baffle designs that use the same relative dimensions as the design from PIP, but Megyesy's design also includes a square top grating — instead of the Patterson's circular solid plate — with dimensions $4D$-by-$4D$. It too is suspended a distance of $D/2$ off the bottom and the baffles extend a small distance into the drain nozzle. Like Patterson, Rousseau [*4*] suggests the use of larger circular plates of $4D$ diameter, suspended a distance of D off the bottom of the tank, compared to the PIP design in which the plate has a diameter of $2D$, located $D/2$ off the bottom.

Similar to Megyesy [*3*], Waliullah [*5*] recommends a square section of grating ($4D$ by $4D$) that is suspended a distance of $D/2$ off the bottom of the tank, and also puts limits on the grating's $4D$-by-$4D$ size based on the tank diameter. Waliullah also proposes a 4-bladed "cross vortex breaker," similar

Author's note: Information contained in this work has been obtained from sources believed to be reliable. However, neither Eastman Chemical nor the authors guarantee the accuracy or completeness of any information published herein and neither Eastman Chemical nor the authors shall be responsible for any errors, omissions, or damages arising out of use of this information. Note that some of the later design information was not in the non-dimensional Froude Number format and some assumptions may have been made to make that conversion.

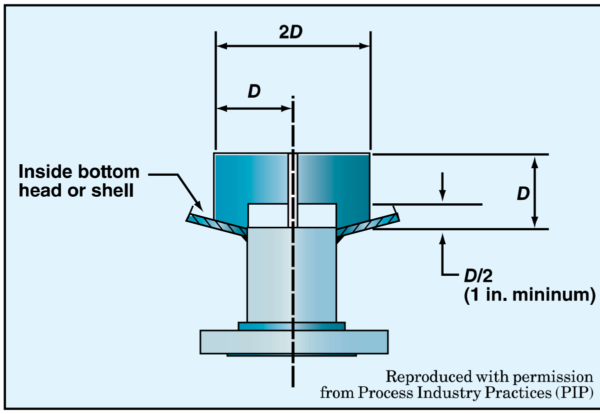

FIGURE 2. This vortex breaker (PIP [2]) consists of a baffle arrangement that suspended or flush with the tank bottom

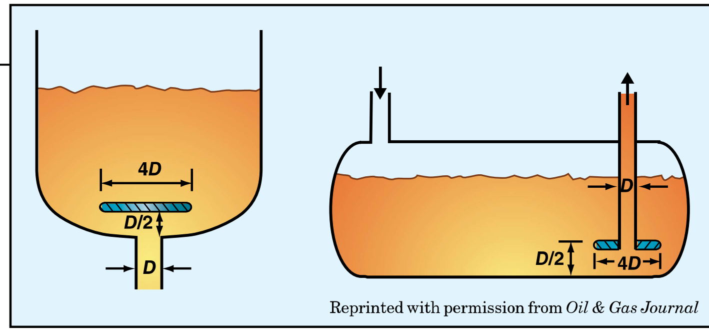

FIGURE 3. Shown here are two alternate vortex breaker designs from Patterson [*1*], for tanks with bottom drainage (left) and vertical-suction discharge (right)

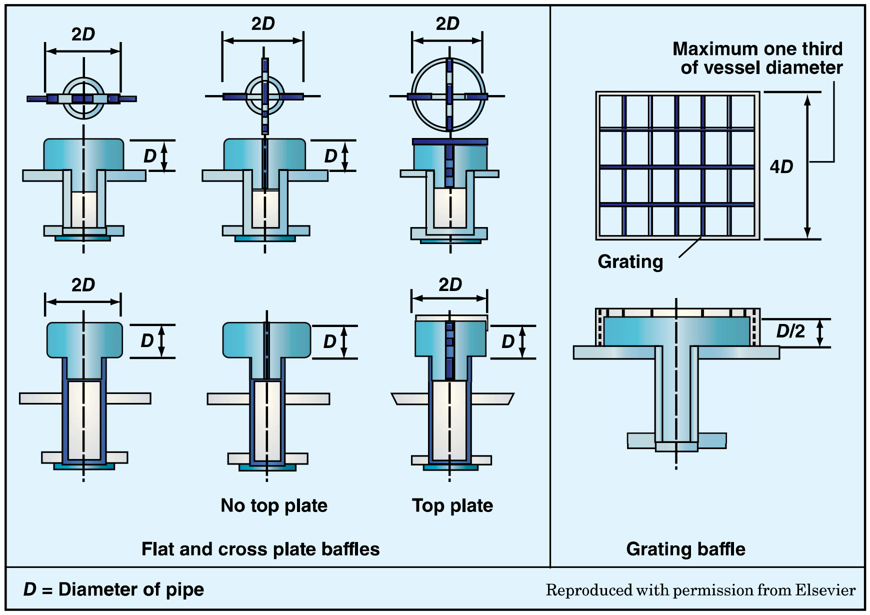

FIGURE 4. The vortex breaker design from Arnold [*10*] combines a 2- and 4-bladed cross pattern with a top plate that is either solid or made from porous grating

to, but larger than the PIP design with a height ranging from 5 in. to 1.25*D*, and a width of 3.5*D* to 5*D*. Kister [*6*] references Patterson [*1*] and Waliullah [*5*] but provides no new data.

McGuire [*7*] repeats the circular 4D plate suspended *D*/2 above the tank bottom, like Patterson [*1*], but also shows a 4-bladed, cross-pattern on top of a nozzle, extended above the tank bottom. However, this reference provides no recommended dimensions. McKetta [*8*] shows a 4-bladed design (4*D* dimension, suspended *D*/2 above the tank bottom) that is within the Waliullah [*5*] range.

The vortex breaker design provided by Voss [*9*] shows a circular plate suspended above the tank bottom of similar size as before, plus an "X-bar" shape that is used to form the 4-bladed cross-pattern. The author says the blades should be "several inches high," rather than related to the drain pipe's diameter. In Figure 4, Arnold [*10*] suggests both the 2- and 4-bladed cross-pattern (2*D* diameter, suspended *D* off the tank bottom, as with PIP [*2*]), plus the grating (4*D* x 4*D* x *D*/2, as with the design by Waliullah [*5*]). Arnold also suggests a combined design shown in Figure 4 (labeled "top plate") of both the 4-bladed cross-pattern and the horizontal top plate. Arnold shows the top plate being made solid as well as from porous grating, as shown. Note that Arnold's blades protrude a short distance down into the drain pipe.

Borghei [*11*] provides a detailed analysis of different configurations of the cross-baffle plate design, varying the design from 8 to 16 baffles, the dimensions of each blade, the distance from the exit pipe, and the height off the bottom. Silla [*12*] references Patterson [*1*], showing the familiar 4-bladed design, with the option of a solid plate or grating on top. The online reference manual provided in Ref. [*13*] from Goulds Pumps covers designs seen before, but also shows a critical submergence trend for vortexing to appear for different flowrates.

Lastly, Rotonics Manufacturing [*14*] shows an "anti-siphon" device online that's also listed as an "anti-vortex" device for side-exit nozzles. It is designed by cutting off half of an extended pipe end, to form a single curved baffle of sorts. One could imagine this "half-pipe" being extended off the bottom of a tank from a bottom-exit nozzle, but offering no construction advantage over the designs reviewed above.

Gas-entrainment potential

Many of the following references (from designs discussed in the literature) discuss "irrotational" or "vortex-less" draining scenarios. It is not clear how the experimental work maintained a non-swirling drain flow (without the addition of baffles or guides) and it is expected that industrial situations would have enough disruptions to make non-swirling flows unrealistic. The discussion that follows on the subsequent references will be treated without regard to whether non-swirling or swirling flows were studied.

Using Perry's "Chemical Engineering Handbook" [*15*] as a starting point, the Kalinske [*16*] work from the early 1940s covered vertical drains and overflow pipes. Perry next points to a 1977 paper from McDuffie [*17*], as well as the 1968 work by Simpson [*18*]. Simpson [*18*] consolidated the Kalinske [*16*] data with the 1938 work by Souders [*19*] on the limits of self-venting, weir-like flow down a drain, and the 1959 theoretical evaluation of critical submergence by Harleman [20]. The Simpson [*18*] graphical comparison used linear-scale axes but plotted non-dimensional parameters of the Froude Number versus the ratio of submergence-to-pipe-diameter.

By comparison, McDuffie [*17*] changed the design chart to log-log scales, which allowed for better resolution at low ranges, and converted the exponential equations to straight lines. McDuffie [*17*] fitted an equation to the Kalinske [16] data (Simpson [18] did not) and noted that the 1971 work of Anderson [21] closely followed Souders' equation [19]. Simpson [22, 23] continued the reviews in 1969 and 1978, but included no new entrainment information.

Equation (1) from Souders [19] predicts when a drain pipe would be running full with no gas entrainment versus the ability of a lower vessel being able to self-vent gas back to the original draining tank. In plotting Equation (1), *Fr* values (Froude Number, defined below) above the equation would imply self-venting occurring, while smaller *Fr* values would suggest flow with no gas entrainment, a condition referred to as running full. Note that this equation is only for *H*/*D* values (liquid height over exit-pipe diameter) less than 0.25. This equation is plotted in Figure 5 (left side).

$$Fr = 2.36\left(\frac{H}{D}\right)^{1.5} \quad (1)$$

where *Fr* is the Froude Number (the dimensionless ratio of inertia to gravity forces), defined as:

$$Fr = \frac{V}{\sqrt{g'D}} \quad (2)$$

$$g' = \frac{g(\rho_L - \rho_G)}{\rho_L} \quad (3)$$

where:

H = the height (or depth) of the liquid's free surface over an exit pipe's entrance, ft
D = the exit pipe diameter, ft
V = the average velocity in drain pipe, ft/s
g = gravity's acceleration constant, ft/s^2
g' = approximates *g* for gas/liquid flows
ρ = the gas-phase and liquid-phase densities, lb/ft^3

The non-dimensional *Fr* is the ratio of the downward drag force of entrained bubbles versus the upward buoyancy force. If the downward drag is not great enough, the bubbles could float upward against the draining pipe flow, and not be caught in the downward flow. The definition is based on the possible case of another liquid resting on top of the draining liquid and being entrained in the drainage flow of the lower liquid. Some use *S* instead of *H* to represent the "submergence" distance of the outlet pipe below the free surface. Users should keep all units consistent.

McDuffie [17] states that when *H*/*D* is above 0.25, and when *Fr* is greater than about 0.3–0.55, gas will become entrained in the draining liquid flow, a condition to be avoided, while for lower *Fr* values the flow will have no vapor entrainment (running full). McDuffie's regression [17] of Kalinske's data [16] is Equation (4) and Harleman's derivation [20] is Equation (5), both related to determining the transition between vapor entrainment versus running full. McDuffie [17] also showed new data that followed Equation (6). Note the similar exponents. McDuffie [17] also reviewed Anderson's 1971 self-venting equation [21] with its leading coefficient of 2.31 being only slightly different from Souders' 2.36 value [19], but with identical exponents.

$$Fr = 4.4\left(\frac{H}{D}\right)^{2.0} \quad (4)$$

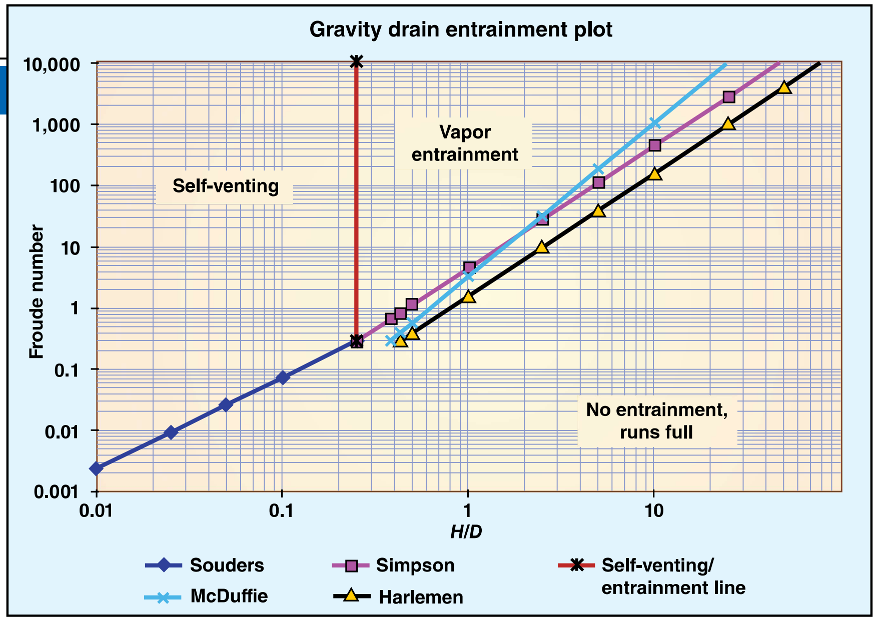

FIGURE 5. A plot of Equations (1, 4, 5 and 6) distinguishes the locations of the three flow conditions: self-venting, vapor-entrainment, and no-entrainment/runs full. Plotting the conditions of a draining tank helps to predict which regime the flow is in and suggest when a vortex breaker is needed to help prevent vapor entrainment

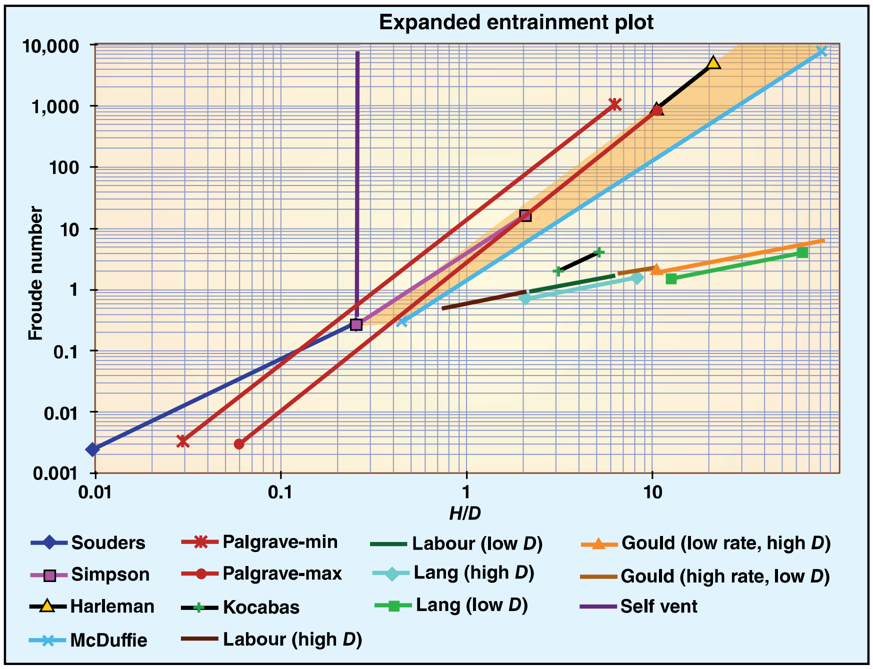

FIGURE 6. Shown here is the expanded master chart with additional rules of thumb added from data gathered from the literature. Disagreement among data sets can be undertood with closer inspection of the original test methods (this is shown in Figures 7–10)

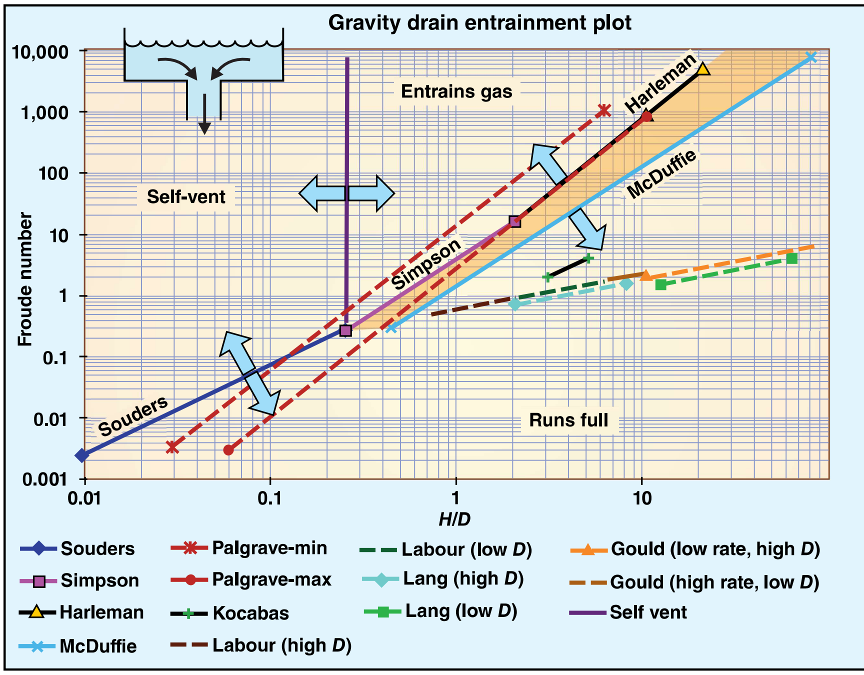

FIGURE 7. This is a repeat of the gravity-drain scenario in Figure 5, but includes all of the additional information, shown as dashed lines to de-emphasize them

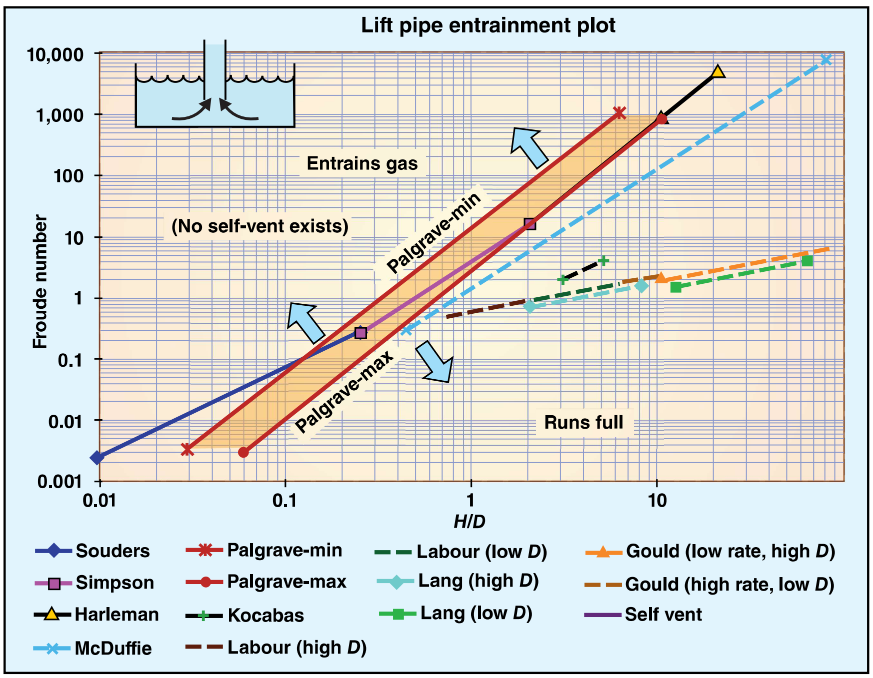

FIGURE 8. This new master chart shows two curves from Palgrave *[28]* and represents tanks that rely on suction-lift discharge pipes. The chart no longer has a Self-vent region because rising bubbles that disengage from the liquid will float up the lift pipe

$$Fr = 3.2\left(\frac{H}{D}\right)^{2.5} \quad \textbf{(5)}$$

$$Fr = 1.6\left(\frac{H}{D}\right)^{2.0} \quad \textbf{(6)}$$

In plotting the design equations, neither McDuffie [*17*] nor Simpson [*18, 22* and *23*] nor even Perry [*15*] labeled all of the three different flow conditions that could exist depending on the tank's operating scenario (found by plotting the Fr and H/D values). Figure 5 shows Equations (1, 4, 5 and 6) using log-log scales with the newly added vertical line at H/D = 0.25 to mark all three possible flow conditions. To the left of H/D = 0.25, only the self-venting and running-full conditions can occur. To the right of H/D = 0.25, the upper region switches to the gas-entrainment condition (hence the need of the vertical divider at H/D = 0.25), while the lower region remains running full.

Note that while the design Equations (4, 5 and 6) may differ by the leading coefficient or exponent, they still cover a similar part of the log-log plot of Figure 5 (Part of this variation could reflect differences in the experimental setup). Users of Figure 5 must decide whether the upper part of the disputed area (formed by the overlapping of Equations (4) and (5), or the lower part via Equation (6), represent a "conservative" design. If the desire is to avoid gas entrainment at all costs, then the lower-bound should be used, as it is a more-conservative scenario.

It should also be pointed out that in all the design equations, the tank's diameter does not appear in the design relationships using the Fr and the H/D notation. The assumption is that this diameter is much larger than the exit pipe's diameter D and thus does not affect the predictions (the actual experiments may have violated this expectation).

As noted earlier, to avoid operational problems associated with vapor entrainment, operation in the regimes labeled "Self-venting" or "No entrainment, runs full" is recommended. This is especially true when vortex breakers cannot be used due to cost considerations or constraints such as a high risk of fouling or plugging.

In an attempt to update the information shown in Figure 5, additional literature searches were conducted but revealed only two new topic areas that were not included previously. The recent publications tend to center around the use of computational fluid dynamics (CFD) modeling to analyze the shape of the "bathtub vortexes" that would lead to gas entrainment in draining tanks. These papers are mostly interested in accurately modeling the shape of the vortex's free surface and predicting when the vertex of the vortex dips down to the entrance level of the drain pipe.

When comparing the references in the CFD papers, all tend to refer to other vortex-shape modeling work (for instance, see Stepanyants [*24*]). In these papers, the main concern is the reduced flow-carrying capability of the drainage pipe when the vortex is occupying a percentage of the open cross-sectional area in that pipe — the issue of gas entrainment seems to be a side concern. The only experimental data set from the CFD papers that is related directly to the air-entrainment work (Lubin [25]) is also quite dated (pre-1980). Converting Lubin's critical height equation [25] to the *Fr* versus *H/D* notation duplicates Equation (5) above from McDuffie [17].

The other group of references found tended to be presented as "rules of thumb" to avoid gas entrainment during tank discharge. These were presented in various dimensional formats, but have been converted here to the consistent non-dimensional *Fr* versus *H/D* form so an expanded "master design chart" presented here can be reviewed. Lang Engineering [26] presents minimum submergence distances versus the average velocity in the outlet nozzle. To make the conversion to the *Fr* versus *H/D* convention, a series of diameters were chosen to calculate a set of non-dimensionalized data to be plotted later.

The online pump-care manual from Goulds Pumps [27] displays the critical submergence versus nozzle velocity, similar to the Lang [26] data, but with an additional flowrate effect on the low end of their data. Again, by calculating a series of pipe diameters, the *Fr* and *H/D* notation can be deduced for later plotting.

Palgrave [28] showed a chart for critical submergence versus flowrate (gal/min). The two curves may be showing an error band for the uncertainty of the transition to gas entrainment. By assuming a series of pipe diameters, the *Fr* and *H/D* values can be calculated.

Labour-Taber [29a] has posted an online white paper by L. Bachus (which cites Ref. [29b] as the data source) that shows two design charts. One is for velocity versus submergence (which will need assumed diameters to continue this comparison) but the other plot, although it appears to have pipe diameter data, is missing the units for the horizontal axis, making it unusable. The units of gal/min are expected to be the units for the missing label on the graph as an alternate presentation of their first graph. Conversion to *Fr* versus *H/D* notation would still be needed.

Kocabas [30] studied gas entrainment in a draining tank evaluating both still-flow versus laterally moving flow, as well as, a solid-bottom versus a porous-bottom. For all of the experimental variations presented in Ref. *30*, only three data points applied to the still-flow/solid-bottom configuration to allow it to be compared to all the other data collected here. Combining the new data reviewed above onto the original master design chart results in a rather confusing Expanded Entrainment Plot, which is shown in Figure 6.

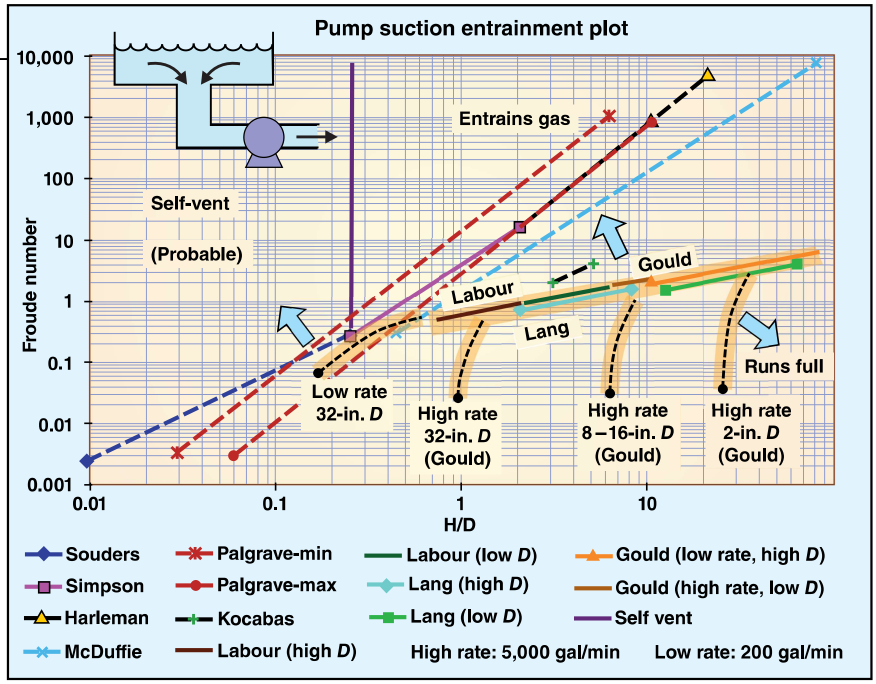

FIGURE 9. This revised master chart for tanks using a pump to discharge liquid from a center drain (rather than discharge being gravity-driven) reflects data from Lang [26], Goulds Pump Care [27] and Labour [29]. The basic data agree but with a different slope for the gravity-driven data. The Self-venting region still exists but due to a lack of data in the cited references, its location is uncertain

Closer review of the added literature revealed that the data presented by Palgrave [28] were only for a "lift pipe" (as shown in the right side of Figure 3), and the information provided by Lang-Goulds-Labour [26, 27 and 29] was all for pump-suction flows, as opposed to gravity-driven, bottom-exiting flows. This implies that Figure 6 actually contains three separate design charts: (1) gravity-driven draining flow from the bottom of the tank; (2) lift-pipe upward-suction flow (perhaps to a pump); and (3) pump-suction flow from the bottom of the tank. Note that Figure 6 is the basis for Figures 7 through 10. As each subsequent scenario is being discussed, the other design curves are included for reference, but dashed to de-emphasize them.

Figure 7 repeats the "gravity drain only" data from Figure 5, but with a shading over the disputed design equations. Note in Figure 7 the short line pointing out the three data points of Kocabas [30], which has a different slope compared to the other gravity-drain data. It is not known why this short curve stands alone when the experimental setup should have matched the previous gravity-drain data.

Figure 8 represents the lift-pipe condition where no self-venting is possible (as the trapped bubbles would just float up the exit lift-pipe), so only two-flow regimes are shown. The band between minimum and maximum conditions may just represent an error-band for uncertainty in the experimental data. The slopes are similar to the original gravity-driven flow equations and the shaded region overlaps the same general region of uncertainty.

Figure 9 shows the remaining data that all have a pump-suction flow condition. Note the three data sets generally agree with a significantly different slope from the gravity-only flow in Figure 7. The self-venting region may exist for this configuration; however, it is not covered by any of the data. The Goulds' data [27] showed "tails" on their data for high rates at different pipe diameters that have been included in the *Fr* versus *H/D* non-dimensional format. High suction rates penalize the operation by reducing the region that ensures no gas entrainment at the lower liquid heights, and those "tails" limit the "running full" coverage. Only by continuing to increase the liquid level can gas entrainment be avoided.

One other data set from the literature has not been discussed. Patterson [*1*] showed limited data for the critical submergence if the tank was recirculating its flow rather than just emptying (draining) its contents. The author stated that an emptying tank needs about three times the critical submergence to avoid gas entrainment compared to a recirculating tank. It is reasonable to assume the returning flow disrupts the formation of a steady vortex of whirlpool and thus allows the free-surface level to be lower (closer to the exit nozzle). However, trying to add his data to the master design chart in *Fr* versus *H/D* notation showed confusing trends (Figure 10), suggesting that his actual experimental setup should be investigated further. A recirculating tank is worthy of further study as it could be a frequently encountered operating condition.

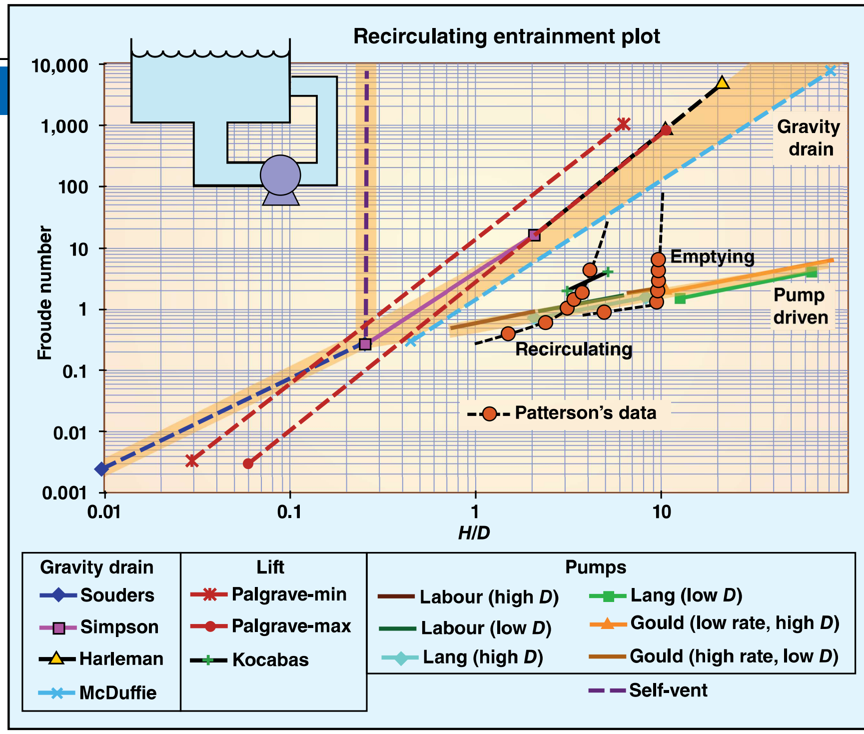

FIGURE 10. Shown is an additional master chart plotted with an approximate depiction of the data provided by Patterson [*1*]. Notice the left-end of the new data has a slope similar to the pump-driven curve discussed previously. No description of the piping arrangement was provided (so it is not clear whether the recirculating piping re-enters the tank on the side or from the top)

Design application

Recently, Eastman Chemical needed to have the bottom nozzle of a new distillation column evaluated for possible gas entrainment. The column was a retrofit with a higher expected capacity compared to the previous column. The bottom nozzle supplies both the thermosiphon reboiler and the bottom draw-off. Operation at previous rates had not exhibited any flow problems. The maximum size of the bottom nozzle was limited due to building structural supports that could not be modified. This maximum nozzle size was below that required for the self-venting flow correlation, per Kister [*6*].

In this application, the use of a vortex breaker could be problematic due to possible flow restriction or plugging. Using the gravity-drain master chart of Figure 5 created in a spreadsheet, operational data for a given design can be converted into the non-dimensional format and plotted on the regime chart (Figure 11).

The recirculation rate, potential nozzle size, and operating level were varied to generate the three design operating ranges. Operation in these ranges (as shown in Figure 11) could be problematic because all except operation at low level indicate the potential for vapor entrainment, and in no situation does it run full. However, since this design uses recirculating flow, Patterson's data [*1*] shown in Figure 10 suggest the actual *H/D* may be equivalent to three times that shown

References

1. Patterson, F.M., Vortexing can be prevented, *Oil & Gas J.*, August 1969, pp. 118–120.
2. Process Industries Practices, http://www.pip.org/
3. Megyesy, E.F., "Pressure Vessel Handbook," 6th Ed., 1983, p. 300.
4. Rousseau, R.W., "Handbook of Separation Process Technology," 1987, p.151.
5. Waliullah, S., Do-it-yourself vortex breakers, *Chem. Eng.*, May 1988, pp.108–109.
6. Kister, H.Z., "Distillation Operation," 1990, pp. 90–94.
7. McGuire, J.T., "Pumps for Chemical Processing," 1990, p. 268.
8. McKetta, J.J., "Encyclopedia of Chemical Processing and Design," 32, 1993, p.113.
9. Voss, J., and others, "Cleaning and Cleaning Validation: A Biotechnology Perspective," 1995, pp. 19–23.
10. Arnold, K., Stewart, M., "Surface Production Operations," Vol. 1, 2nd Ed., 1998, p. 112.
11. Borghei, S.M., Partial Reduction of Vortex in the Vertical Intake Pipe, 4th International Conf. Hydro-Sci & -Engr, Korea, 2000.
12. Silla, H., "Chemical Process Engineering, Design and Economics," 2003, pp. 273–280.
13. Goulds Pumps, On-line Piping Design Section 02, accessed at: www.gouldspumps.com/pag_0006.html.
14. Rotonics Manufacturing's online products list, accessed at http://www.rotonics.com/tanks/accessories/RMI%20Tank%20Accessories.pdf .
15. Perry's "Chemical Engineering Handbook," 6th Ed., 1984, McGraw-Hill, pp. 5–44.
16. Kalinske, A., Hydraulics of Vertical Drain and Over-Flow Pipes, University of Iowa Studies in Engineering, Bulletin No. 26, 1941, pp. 26–40.
17. McDuffie, N.D., Vortex free downflow in vertical drains, *AIChE J,* Vol. 23 (1), Jan 1977, pp. 37–40.
18. Simpson, L., Sizing piping for process plants, *Chem. Eng.*, June 17, 1968, pp. 192–214.
19. Souders, M., Huntington, R.L., Corneil, H.G., Emert, F.L., Performance of bubble-plate columns, froth heights and pressure differentials, *Ind. Eng. Chem.*, Vol. 30 (86), 1938.
20. Harleman, D.R.F., Morgan, R.L., Purple, R.A., Selective Withdrawal from a Vertically Stratified Fluid, 8th Congress International Assn. for Hydraulic Research, 10-C-1, Montreal Canada, Aug. 1959.
21. Anderson, A.G., Vaidyaraman, P.P., Chu, C.S., "Hydraulics of Long Vertical Conduits and Associated Cavitation", U.S. E.P.A. Water Pollution Control Research Series, 11034 FLU 06/71, 1971.
22. Simpson, L., Process piping: Functional design, *Chem. Eng./Deskbook Issue*, April 14, 1969, pp.167–181.
23. Simpson, L., Weirick, M., Designing Plant Piping, *Chem. Eng./Deskbook Issue*, April 3, 1978, pp. 35–48.
24. Stepanyants, Y.A., Yeoh, G.Y., Stationary bathtub vortices and a critical regime of liquid discharge, *J. Fluid Mech,* V604, 2008, pp. 77–98.
25. Lubin, B.T., Springer, G.S., The formation of a dip on the surface of a liquid draining from a tank, *J Fluid Mech*, Vol. 29 Part 2, 1967, pp. 385–390.
26. Lang Engineering White Paper by Flint Evans, entitled Rules to Follow to Avoid Pump Problems, no date.
27. Goulds Pumps: Pump Care Manual, ITT Industries Ed, 9-2002, accessed at: http://www.gouldspumps.com/download_files/literature_misc/PumpCareManual.pdf .
28. Palgrave, R., "Troubleshooting Centrifugal Pumps & Their Systems," Elsevier, 2002.
29. Labour Taber white paper by Larry Bachus, reproducing information from "Know and Understand Centrifugal Pumps," by L Bachus, A Custodio, Elsevier 2003.
30. Kocabas, F., Unal, S., Unal, B., A neural network approach for prediction of critical submergence of an intake in still water and open channel flow, *Computers & Fluids,* 37, 2008, pp. 1040–1046.

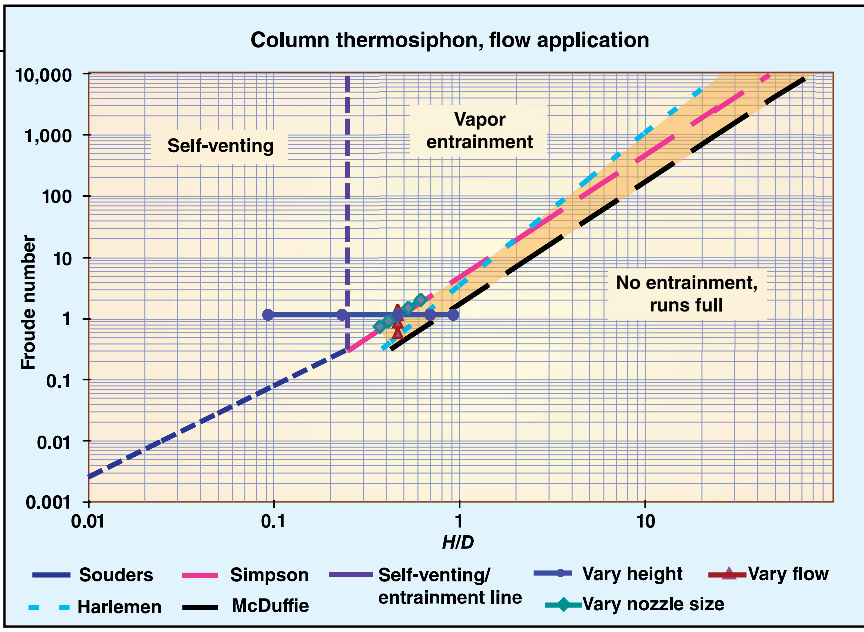

FIGURE 11. Using production and design data from an actual tank, it is possible to block out the three possible operating ranges — Self venting; No entrainment, Runs full; and Vapor entrainment — as a function of different liquid heights and flowrates. This master design chart lets the user see the operating conditions under which the tank faces the increased risk of vapor entrainment

in Figure 11. This would shift operation to the right (into the favorable "No entrainment, Runs full" regime), but would be based on inconsistent recirculating data as compared to the other pump and gravity-flow data.

Because this correlation has not been applied much to date within Eastman, and this particular application fell into a potential problem area, a removable vortex breaker was fabricated for the column and started up without any problems. Eastman has begun routinely using this correlation to check the need for vortex breakers in equipment designs. ■

Edited by Suzanne Shelley

Authors

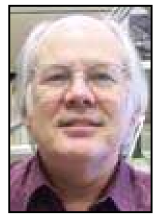

Steve G. Rochelle, P.E., has been is an engineering associate with Eastman Chemical Co. (P.O. Box 431, B-54D, Kingsport, TN 37662; Phone: 423-229-6172; Email: rochelle@eastman.com) since 1976. He holds a Ph.D. in engineering mechanics from Tennessee Tech, is a professional engineer in Tenn. and South Carolina, and specializes in computational fluid dynamics.

Marvin T. Briscoe, Jr. has been a senior engineer with Eastman Chemical's Process Engineering Dept. (Phone: 423-229-1274; Email: mbriscoe@eastman.com) since 2005. He holds an M.S.Ch.E. from the University of Louisville, and specializes in process and equipment design, troubleshooting, and debottlenecking.